NDT&E International 63 (2014) 11–20

Contents lists available at ScienceDirect

NDT&E International

journal homepage: www.elsevier.com/locate/ndteint

Non-destructive evaluation of cracks in massive concrete using normal dc resistivity logging

E. Taillet [a,b,*], J.F. Lataste [a,1], P. Rivard [b,2], A. Denis [a,3]

[a] Laboratoire I2M, Université de Bordeaux, Avenue des facultés, Bât.18, 33405 Talence Cedex, France
[b] Département Génie Civil, Université de Sherbrooke, Sherbrooke, QC, Canada J1K 2R1

ARTICLE INFO

Article history:
Received 17 May 2013
Received in revised form
20 November 2013
Accepted 6 January 2014
Available online 16 January 2014

Keywords:
Normal resistivity
Borehole logging
Concrete
Cracks

ABSTRACT

Discontinuities are one of the most harmful damage to the durability of concrete structures. Currents approaches are limited to assessments of surface damages, even if non-destructive methods appear to be effective for the detection and the location of cracks. That is why, these methods might be unsuitable for investigation of massive concrete body as dams and locks. Present works aim at the presentation of new results with electrical resistivity to study damages within concrete structures. In this article, the electrical resistivity focused on the study of cracks and discontinuities (concrete joints, interfaces…) in massive concrete structures by measurements done in preexisting boreholes. The used array is the normal dc resistivity logging. The study presents numerical and experimental results. First, modeling allows correcting experimental data. Then, development shows the sensitivity relatively to the discontinuity characteristics (aperture and the resistivity contrast between the discontinuity and the concrete). The tests on a real structure are carried out to define the methodology for on-site measurement. Results support the modeling.

1. Introduction

Aging massive concrete structures is a major problem due to the decay of concrete properties and performance over time. The structures repair is often less expensive than the reconstruction; it is important to make a diagnosis with non-destructive testing (NDT) methods. To reduce the maintenance costs of structures, it is required to detect, locate and characterize the altered zones especially in terms of cracking. The presence of discontinuities promotes the infiltration of water and has an accelerating effect on the concrete deterioration. The focus is notably put on interfaces linked to implementation conditions (workmanship) which are classic default zones. Due to casting process, these faults generally have sub-horizontal orientation. The contact zone between rock and concrete is also considered on these constructions.

Today, the techniques of acoustic and optical imaging are among the only means to explore inside the massive concrete body. They are based on measurements done in boreholes done through the construction, as logging. They give partial information of the damage with an image of the borehole wall. Apparent information provided by these techniques are insufficient to establish a complete diagnosis of the degradation state of the structure. The research presented in this article intends to provide additional information to the techniques already used. So, this work is directed towards the exploitation of the electrical behavior of concrete including its electrical resistivity. Indeed, in previous studies of surface resistivity method has demonstrated its sensitivity to factors indicative of an alteration (change in porosity, presence of gaps, etc.) [1,2]. One wants to investigate damages in the volume beyond the borehole space.

The electrical resistivity surface methods are limited due to their shallow investigation depth and their resolving power. The increase in the spacing between two electrodes can probe deeper but the resolution decays [3]. In an investigation of the internal structure, discontinuities in a concrete body are assessed with electrical resistivity measurements made via pre-existing boreholes: the normal dc resistivity logging.

Abbreviations: a, additional constant; A, current electrode; AM, distance between A and M (m); B, current return electrode; $C_{a/m}$, contrast between the apparent resistivity and the resistivity of the borehole fluid; $C_{t/c}$, contrast between the concrete resistivity and the crack resistivity; $C_{t/m}$, contrast between the concrete resistivity and the resistivity of the borehole fluid; D_b, borehole diameter; F, formation factor; h, crack aperture; I, intensity; m, cementation factor; M, potential electrode; M_x, electrode name remote of "x" inch from A; N, reference electrode; ϕ, porosity; r, Radius; V, electrical potential; ρ, resistivity; ρ_a, apparent resistivity; ρ_{a1}, apparent resistivity corrected of the surface effect; ρ_{a2}, apparent resistivity corrected of the borehole effect; ρ_c, crack resistivity; ρ_m, resistivity of borehole fluid; ρ_t, concrete resistivity

* Corresponding author at: University of Sherbrooke, Department of Civil Engineering, Sherbrooke, QC, Canada J1K 2R1. Tel.: +1 33 6 67 64 09 28.
E-mail addresses: elodie.taillet@usherbrooke.ca, elodie.taillet@gmail.com (E. Taillet), jean-francois.lataste@u-bordeaux1.fr (J.F. Lataste), patrice.rivard@usherbrooke.ca (P. Rivard), a.denis@i2m.u-bordeaux1.fr (A. Denis).
[1] Tel.: +33 5 40 00 88 42.
[2] Tel.: +1 819 821 8000x63378.
[3] Tel.: +33 5 40 00 26 19.

0963-8695/$ - see front matter © 2014 Elsevier Ltd. All rights reserved.
http://dx.doi.org/10.1016/j.ndteint.2014.01.001

In the early 20th century, borehole logging tools, such as resistivity, sonic, nuclear logging tools were developed for oil prospection to obtain continuous record of a formation's rock properties [4,5]. The first studies have been focused on the response of an electrical logging tool facing interfaces by analytical calculations [6–8]. With the evolution of the borehole logging applications, scientists have developed analysis and methods designed to investigate thin sand and clay beds of few decimeters [9,10]. Then, Yang and Ward showed the relation between electrodes spacing and layer thickness [11]. The development of numerical methods allows studying the electrical logging capacities and developing methods to interpret thin beds in a single borehole [12] or two boreholes [13].

In a different context, our study continues this scientific work in developing the capacity of borehole techniques and provides another tool to characterize discontinuities. This paper deals with the application of a normal electrical probe in structures poured in concrete layers (sub-horizontal planes). The probe sensitivity against weakness zones (joints, cracks, interfaces) is determined. Different spacings between the electrodes were used to obtain information on different depths of investigation. The information combination allows having a survey through a lateral plane along the borehole. The study is based on a 2D-axisymmetric modeling and inversion calculation to characterize the tool response against cracks. Investigation measurements recorded on a massive structure are presented to support the modeling results and to validate the method reliability.

2. Electrical resistivity logging: Normal probes

2.1. Electrical resistivity concepts

In concrete, the current circulation is primarily linked to the pore solution found in the cement paste, so called electrolytic conduction [14]. Thus, the electrical resistivity is sensitive to porosity variation or preferential paths for fluid flow within material (i.e. cracks).

Archie determined an empirical relationship between the electrical resistivity and the porosity in a saturated rock [15]. This relationship was generalized to unconsolidated rock and marine sands by Atkins and Smith [16] (Eq. (1))

$$F = a \times \phi \times \exp - m \tag{1}$$

where F is the formation factor, a is defined as an additional constant, ϕ is the porosity of medium and m is the cementation factor. In concrete, F is defined as the ratio of the measured resistivity of the concrete to the resistivity of the cement paste, and ϕ, the volume fraction of the paste in the concrete.

Previous studies conducted with a four-probe square array have shown the capability of the electrical resistivity method to detect and locate resistant or conductive cracks concrete [2]. For massive concrete structures such as dams, where the zones of interest are too deep, surface methods do not appear to be suitable. Many authors have shown that subsurface electrodes permit far greater accuracy and resolution than can be obtained from surface-only arrays [17,18].

2.2. Normal device

Used in the oil industry, the logging tool is inserted in a borehole with an armored cable. The probe is raised with recording speed to obtain continuous series of measurements as a function of depth. The electrical normal logging is a device which has a current electrode A and a potential electrode M located in the borehole and a current return electrode B and a reference electrode placed on the surface N (Fig. 1). B and N are considered to be infinite and the device is compared with a surface pole–pole array [19].

In an infinite homogeneous medium, the potential drop is the same in all directions and can be represented by many spheres centered at A. By integrating an entire volume of ground, the potential drop is described by Eq. (2)

$$-dV = ((\rho \times I)/(4 \times \pi \times r \exp 2)) \times dr \tag{2}$$

where dV is potential difference (V), ρ is resistivity (Ω m), I is current intensity (A) and r is radius (m). AM spacing is usually fixed to 16″ (0.4 m) and called the short normal or to 64″ (1.6 m) called the long normal. There are also other probes such as the very short normal with a spacing of 8″ (0.2 m) and the middle normal with a spacing 32″ (0.8 m). The increased distance allows probing on larger investigation volumes of material. Its radius is defined as the distance at which the measurements are sensitive. For a normal probe, 50% of the electrical signal generated by the electrode A is obtained at a distance equal to $2AM$ [20]. However, this value is controversial [21].

For an isotropic and homogeneous medium, the measurement of the resistivity is the true resistivity. However, for a heterogeneous medium, this measurement is called the apparent resistivity, ρ_a. The apparent resistivity is the average of the resistivity for a given investigation volume. This value depends on the nature of the material, the water content, environmental conditions and the electrode spacing.

Normal logging applications provide qualitative and quantitative information about geological formations when the thicknesses of formations are larger than the tool's size. Physical properties and geometry layers govern the measurement analysis. For a

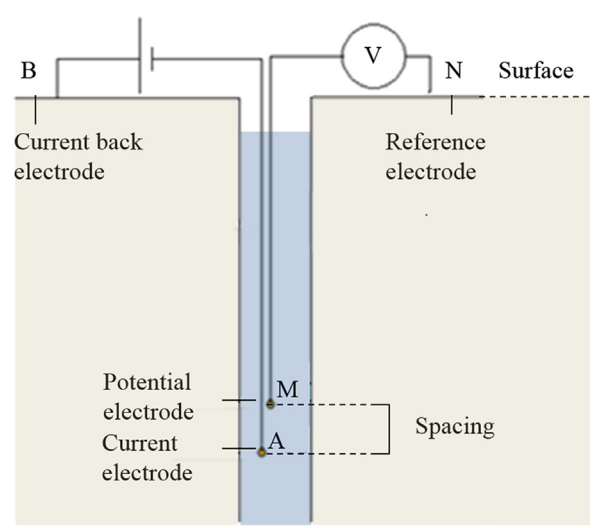

Fig. 1. Normal logging device.

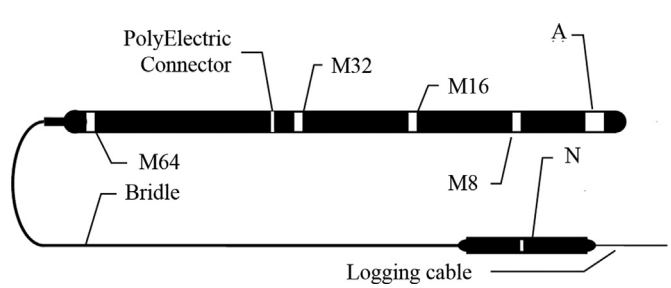

Fig. 2. 2PEA-1000 probe (Mount Sopris Instrument [22]).

conductive layer, a resistivity decrease is observed. Geometric limits are overestimated by an amount equal to the spacing $AM/2$.

2.3. Measurement probe specificities

The 2PEA-1000 probe was used for this study (Fig. 2) [22]. It allows, in a single operation, obtaining several measurements such that apparent resistivity (normal device). Only the normal device is discussed in this paper. The probe has an electrode A, source of DC current, and four measurement or potential electrodes M8, M16, M32 and M64 given four different depth of penetration around the borehole. The probe is connected to the winch system with a bridle made of insulating material to avoid any interaction with the metal parts of the device. The data are then collected through the data acquisition system MGX II © for converting analog information to digital information. Measurements, made during the ascent of the tool, are collected and displayed with the software MSlog © [23].

Electrode B is planted in soil away from borehole to have a good electrical coupling. The N-electrode is located at the connection between the bridle and the winch cable at 9.35 ± 0.1 m away from the injection electrode. N is considered to be at infinity by Mount Sopris Instrument Company.

The assembly must be immersed in the borehole. This technique is not suitable in dry holes. If the N-electrode is emerged, no measurements are recorded. The size of the device is a major constraint so the length of the borehole must be longer than 9.35 m. In addition, the diameter of the borehole should be greater than 50 mm (probe diameter).

3. Numerical results

3.1. Model definition

The aim of this section is to model an electrical probe and to understand how the current is distributed around the borehole. The finite element software Comsol3D © was used [24]. Simplified assumptions were made. The problem was reduced to a 2-D axisymmetry model with an axis of symmetry at the center of the borehole. Moreover, it was assumed that the medium is homogeneous, isotropic and infinite. The model was defined according to three sub-areas: the tool (electrode and insulating parts of the probe), the borehole fluid and the surrounding concrete structure.

In this system, the boundary and interfaces conditions are implemented. We use conditions on insulating surfaces of the mandrel and the contact surface (air/concrete), and a zero potential at the limits of the concrete located to infinity. In addition, a DC current source of 1 A is applied to the surface of the electrode A. The conditions of continuity of the potential and current conservation were imposed on different interfaces. In a homogeneous, isotropic and infinite medium, the resistivity of the borehole fluid ρ_m is equal to the resistivity of the concrete, ρ_t. The apparent resistivity, ρ_a should be equal to the imposed resistivity in model. To validate the model, an error was calculated for each AM spacing (Eq. (3))

$$E(\%) = ((\rho_t - \rho_a)/\rho_t) \times 100 \tag{3}$$

After testing several model sizes, a model of 20 m of length by 50 m of height was selected. The error is less than 5% for M8, 2.5% for M16, 2% for M32 and M64. It can be seen that the modeling errors come from the numerical errors, configuration errors and probe effect errors.

This model has a mesh made of triangular elements side ranging from 0.001 to 1 m. The spacing between nodes is equal to 0.001 m on either side of the current source to ensure the accuracy of the injection point. The maximum number of nodes is 95,888 with computation time estimated to 30 s for each position of A.

3.2. Modeling corrections

Modeling shows bias in the apparent resistivity measurements associated with the effect of the surface and especially with the effect of borehole when we imposed a contrast between the borehole fluid and the concrete.

The first apparent resistivities strongly differ from the true resistivity when approaching the surface. To correct this surface effect, the calculations were made according to the theory of images. The error is due to the addition of a secondary source in the measurement, i.e. another image of the source A, relative to the ground surface [25]. To correct apparent resistivities, measurements must be recalculated with Eq. (4)

$$\rho_{a1} = (\Delta V/I) \times (4 \times \pi/(1/(|Z_a - Z_m|) - 1/(|Z_a - Z_n|) + 1/(Z_a + Z_m) - 1/(Z_a + Z_n))) \tag{4}$$

where ρ_{a1} the apparent resistivity corrected of surface effect, ΔV is the potential difference (V), I is the current intensity (A), Z_a is the current electrode depth, Z_m is the potential electrode depth and Z_n is the reference electrode depth. Modeling showed that the surface effect does not explain measurement errors found in this paper. The application of the surface correction equation is effective for the data between 0 and -3 m (M8 and M16 spacings), and for the data between 0 and -8 m (M32 and M64 spacings). Beyond these

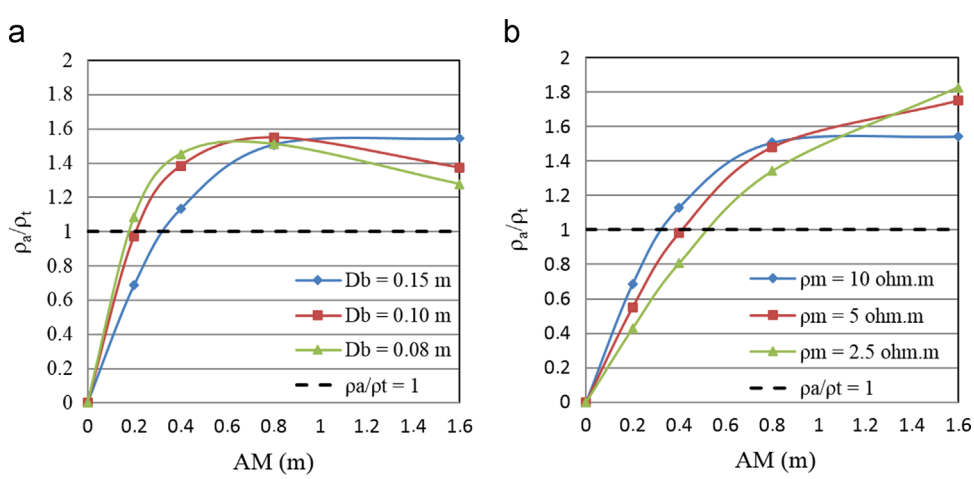

Fig. 3. Ratio of the apparent and true resistivity (ρ_a/ρ_t) versus the distance between the A and M electrodes (AM) (a) for different borehole diameters D_b and a given fluid resistivity, $\rho_m = 10\ \Omega$ m; (b) for different fluid resistivity (ρ_m) and a given borehole diameter, $D_b = 0.15$ m.

depths, the correction has no impact on the measurements. The error came from another artifact.

The diameter of the borehole (D_b) and the resistivity of the borehole fluid (ρ_m) are two parameters that influence the measurements. An analysis of the impact on data modeling is conducted (Fig. 3). Theoretically, the borehole influence decreases away from the point of current injection (A). Thus, for large spacing, ρ_a is close to ρ_t and ρ_a/ρ_t tends toward 1. However, Fig. 3 shows that some ratio ρ_a/ρ_t differ from 1, indicating that the apparent resistivity is greater than the true resistivity value of the concrete imposed to the model. Similar results have been found in a study concerning a soil investigation for tunneling [26]. The variation of the fluid resistivity and the variation of borehole diameter bias the tool response. Moreover, Serra [4] proved the effects of borehole are more important on the tool response when the hole is large and the fluid resistivity is low. In this study, this assumption is verified for large spacings (M64) but is not the case for small spacings (M8/M16).

This effect can be quantified with an analytic calculation developed by Wait [27]. The first corrections on the effect of the borehole fluid and its diameter were made by Schlumberger [28]. From these primary analysis, Scott developed a FORTRAN algorithm to correct logs obtained from all types of normal probe. In each application, there are two simplified assumptions [29]. First, the thickness of the bed is assumed to be infinite (at least 10 times larger than the spacing between electrodes). Second, the invasion of borehole fluid into the formation is considered as negligible. Indeed, the borehole fluid is the same as the fluid that saturates the structure because the studied boreholes are old.

Using the modeling data, we decided to develop a specific equation to the configuration of the probe (Eq. (5)) [30]. The method of nonlinear multiple regression was used. The logarithm of $C_{t/m}$ (the contrast between the resistivity of concrete and the resistivity of borehole fluid) depending on logarithms of $C_{a/m}$ (the contrast between the apparent resistivity and the resistivity of borehole fluid) and the relationship between AM and D_b were chosen. Ln ($C_{t/m}$) is considered as the dependent variable while Ln ($C_{a/m}$) and Ln (AM/D_b) and their product are taken as independent variables.

$$\begin{aligned}\mathrm{Ln}(C_{t/m}) = &-0.00075 \times \mathrm{Ln}\,(C_{a/m})^4 + 0.02299 \\ &\times \mathrm{Ln}\,(C_{a/m})^3 - 0.06325 \times \mathrm{Ln}\,(C_{a/m})^2 + 1.11849. \\ &- \mathrm{Ln}(C_{a/m}) + 0.01300 \times \mathrm{Ln}\,(AM/D_b)^4 - 0.10401 \\ &\times \mathrm{Ln}\,(AM/D_b)^3 + 0.21102 \times \mathrm{Ln}\,(AM/D_b)^2 \\ &0.07903 \times \mathrm{Ln}(AM/D_b) + 0.00069 \times \mathrm{Ln}\,(C_{a/m})^4 \\ &\times \mathrm{Ln}(AM/D_b) - 0.01209 \times \mathrm{Ln}\,(C_{a/m})^3 \\ &\times \mathrm{Ln}(AM/D_b) + 0.02144 \times \mathrm{Ln}\,(C_{a/m})^2 \times \mathrm{Ln}(AM/D_b) \\ &-0.10210 \times 2 \times \mathrm{Ln}(C_{a/m}) \times \mathrm{Ln}(AM/D_b) \\ &-0.00624.\ \mathrm{Ln}\,(AM/D_b)^4 \times \mathrm{Ln}(C_{a/m}) + 0.03798 \\ &\times \mathrm{Ln}\,(AM/D_b)^3 \times \mathrm{Ln}(C_{a/m}) + 0.01112. \\ &\mathrm{Ln}\,(AM/D_b)^2 \times \mathrm{Ln}(C_{a/m}) \end{aligned} \tag{5}$$

Fig. 4 shows the error percentage of uncorrected and corrected data versus the model for the four spacings. The model has a concrete resistivity equal to 200 Ω m, a fluid resistivity equal to 10 Ω m and a borehole diameter of 0.15 m. The calculation of the error percentage is obtained by Eq. (3). The corrective equation yields realistic data with an error less than 5%. However, according to the contrast $C_{t/m}$, the AM spacing and the borehole diameter, this error can reach up to 10% without exceeding it. This equation is valid for this geometry of probe, i.e. with the dimensions of the electrodes and its own diameter.

In the follow of paper, the apparent resistivities are only corrected of the borehole effect (ρ_{a2}).

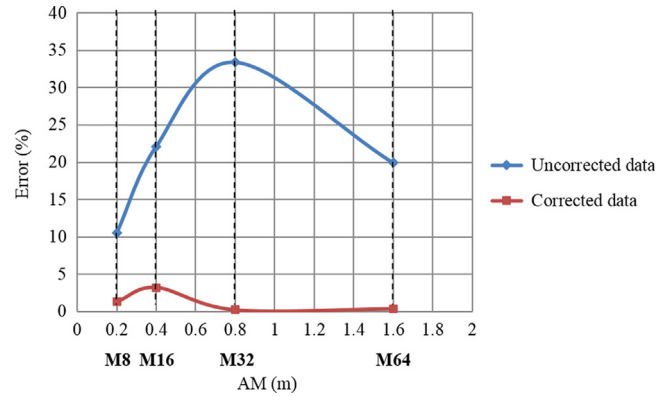

Fig. 4. Percentage of error existing between the imposed resistivity in model and the uncorrected and corrected apparent resistivity versus the distance between the A and M electrodes (AM).

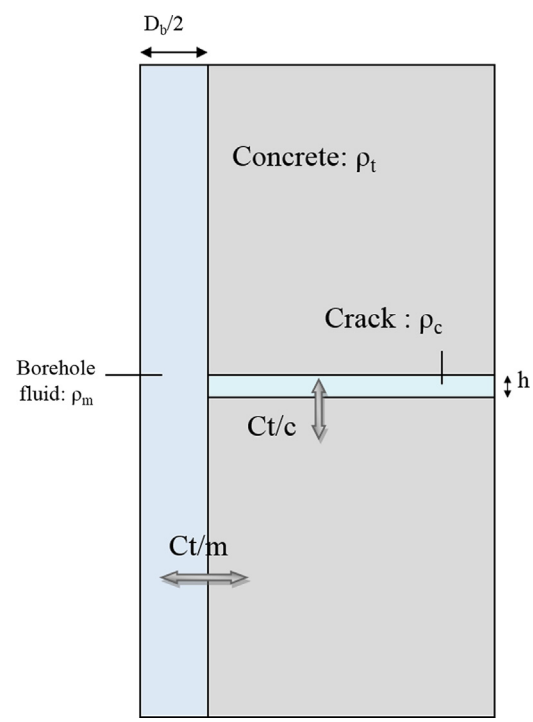

Fig. 5. Schema of cracked model.

3.3. Sensitivity studies on the crack parameters

We introduce a horizontal conductive crack with an aperture h, a resistivity ρ_c, and an infinite extension, located at mid-depth (Fig. 5). In modeling, we considered the resistivity contrast between different mediums. $C_{t/m}$ is the contrast between concrete resistivity and the resistivity of the borehole fluid, and $C_{t/c}$ is the contrast between concrete resistivity and the resistivity of the crack.

In this section, we investigate the disturbance generated by a conductive crack into the concrete medium. We calculated a relative variation right to the crack, i.e. a resistivity decrease in percentage. The calculation is the same as Eq. (3) with ρ_t and ρ_{a2} right to the crack. In the following figures, we consider 1% noise field. This value was assessed by on site measurement repeated with only few seconds′ delay in a single borehole with the same conditions. The noise was calculated as the average on the log of the coefficient of variation of six resistivity measurement on each point of the electrical log.

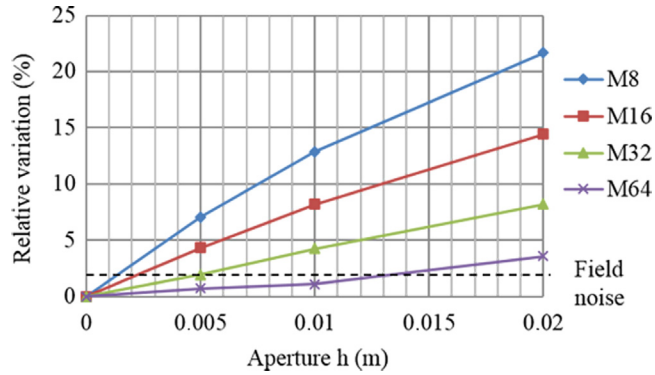

Fig. 6. Influence of the crack aperture (h) for each spacing (AM from 8″ to 64″) and with a resistivity contrast between the concrete and the crack, $C_{t/c}$, equal to 10.

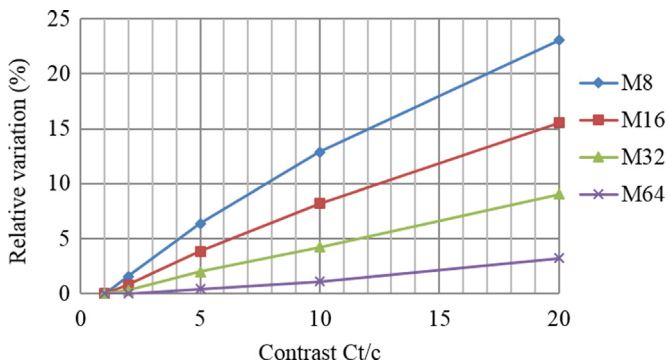

Fig. 7. Influence of the resistivity contrast between the concrete and the crack ($C_{t/c}$) for each spacing (AM from 8″ to 64″) and with a horizontal crack aperture h=0.01 m.

Fig. 6 shows the relative variation as a function of the crack aperture h, with a borehole diameter, D_b equal to 0.1 m, $C_{t/c}$ equal to 10 and $C_{t/m}$ equal to 10.

The relative variation is significant for large apertures and small spacings. It was assumed that the relative variations below 1% (field noise) do not explain the presence of cracks. For a large spacing (M64), a crack aperture equal to 1 cm (with $C_{t/c}$=10) was not perceptible (Fig. 6).

Fig. 7 shows the relative variation as a function of the resistivity contrast between the crack and the medium $C_{t/c}$, for a borehole diameter of 0.1 m, a crack aperture of 0.01 m and $C_{t/m}$ is equal to 10. The conclusion is similar to the one made for the aperture. The relative variation right to the crack is important when the contrast is great and the spacing is small. For a thin crack (h=0.01 m), a contrast between 1 and 2 gives no information. For a contrast between 2 and 3, only M8 and M16 spacings provide significant relative variations. For a contrast between 3 and 7, M32 spacing provides additional information. The information of the four spacings is used when the contrast is up to 7.

The tool response depends on the crack aperture, the contrast with the concrete and the used spacing. The crack detection is based on its representation in a volume of investigation (2AM). A thin crack (h=0.01 m) with low contrast ($C_{t/c}$=2) cannot be detected in a volume with a radius equal to 2 × M32 (Fig. 7).

3.4. Measurement inversion

The inversion is an iterative method used to build a model with true resistivity from modeling or field data in corrected apparent resistivity. The model response must agree with the measured data [31]. However, it would be incorrect to use it as a final image of the true resistivity because it may lead to many solutions. Fig. 8 shows an example of an inversion result made from modeling data in a single-borehole electrical configuration (Software Res2DINV © [32]). The initial concrete model (20 Ω m) has a horizontal infinite crack at 2 m with an aperture of 0.01 m, and a resistivity of 2 Ω m. The borehole fluid resistivity is 2 Ω m. The image (a) is the representation of the initial model response obtained by modeling. It consists of corrected apparent resistivity measurements spaced 0.1 m. The image (b) is the estimated model obtained from inversion method in true resistivity.

The image of apparent data provides little information. The resistivity varies from 16 to 20 Ω m. The low resistivity zone is located at 2 m. The inversion interpretation gives more information about the discontinuity. At a depth of 2 m, the low resistivity zone varies from 4 to 10 Ω m with a thickness of 0.2 m and a lateral extent of 1.6 m. The pseudo-depth 0.2 and 0.4 m indicates a resistivity between 4 and 6 Ω m. This conductive zone is located between higher resistivity zones. These resistivities are even higher when the contrast between the crack and the environment is important. For a pseudo-depth equal to 0.2 m and at 1.4 m from the low resistivity zone, the medium resistivity is approximately 20 Ω m.

The inversed data give quantitative information about the true resistivity of the crack ρ_c ±3 Ω m and the true resistivity of the medium ρ_t with an error of 5%. The information accuracy is given by the low spacing (M8 and M16) and a high contrast.

The crack size (0.02 m) is less than the mesh (0.10 m) used by the inversion method. Therefore, the inversion does not seem to be an adapted approach to characterize the crack aperture. In addition, the inversion method brings artifacts, such as a resistivity increase near the crack. These results show that the domain analysis should not depend only on the inversion method but should also take into account the apparent resistivity variations for each spacing.

4. Experimental results

4.1. Experimental site

The aim of this step is to validate the tool sensitivity with field survey. The measurements were conducted on a large concrete hydraulic structure built about 50 years ago (Fig. 9a). The structure is composed of massive concrete with a maximum size of aggregates of 150 mm. Only 30% of aggregates have a diameter over 75 mm. The nature of these aggregates is a crushed clayey limestone. The concrete tested a compressive strength varying between 20 and 45 MPa. There is little or no reinforcement in the structure. The presence of rebars or metal objects is not recommended. The concrete is considered as saturated because the structure is relatively old and is in contact with the seaway canal. The structure is adjacent to an embankment where the return electrode was planted.

The bedrock is a highly fractured Ordovician shale from the Utica formation. Thus, it has many sub-horizontal natural fractures along the schistosity of the rock.

The measurements were made in four boreholes that have been previously drilled down to the bedrock (Fig. 9b).

4.2. Raw and corrected data

The data come from geophysical surveys conducted during summers 2010 and 2011. The measurements were performed during the recovering of the tool, with a recording speed of about 0.60 m/min. The sampling step was fixed to 0.05 m. The presented results take in account the measurements made from the bottom of the borehole, up to 10.5 m. This is the depth from which the N

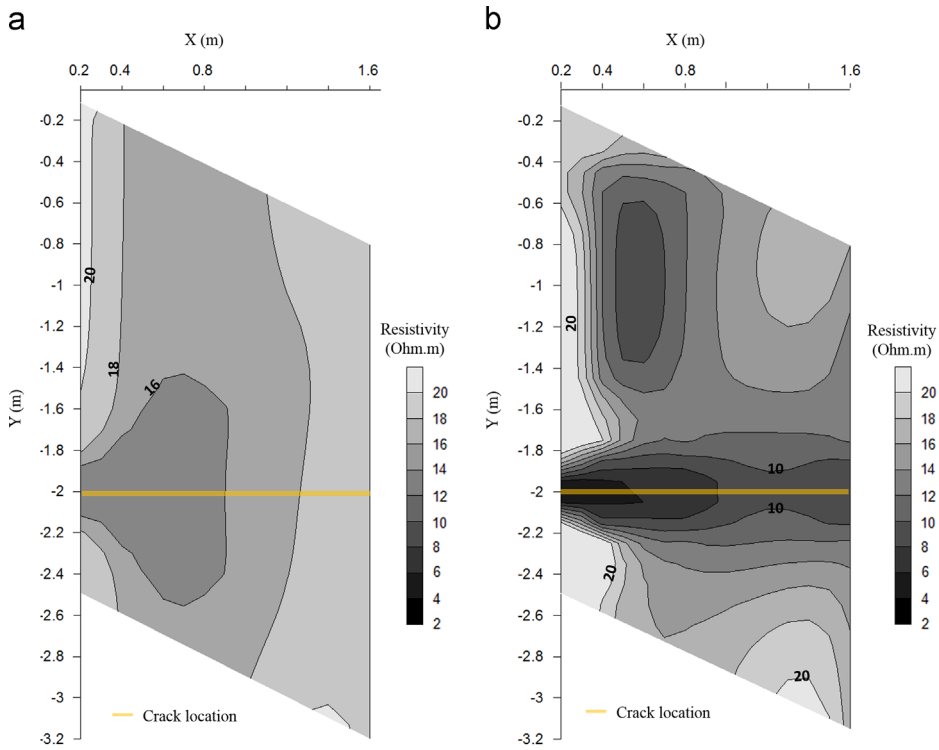

Fig. 8. Resistivity pseudo-section from a single-borehole pole–pole configuration: (a) Corrected apparent resistivity (b) inversion result.

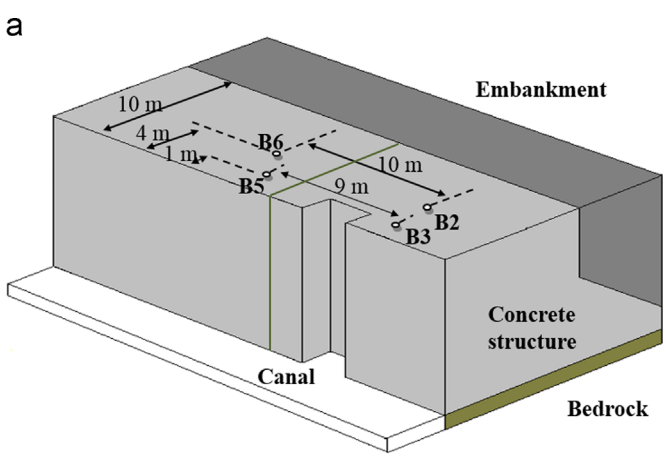

b

	Diameter (mm)	Drilled length (m)
Borehole 2 (B2)	75	14.5
Borehole 3 (B3)	152	16.3
Borehole 5 (B5)	152	15.1
Borehole 6 (B6)	95	14.6

Fig. 9. Experimental site: (a) Schematic representation of the concrete hydraulic structure, (b) geometric information of boreholes.

probe came out of the borehole fluid and is not immerged anymore; it might lead to erroneous results.

Fig. 10 shows raw and corrected data of the borehole B6 for the four electrode spacings. The field data were corrected with the developed equations (Eq. (5)). The borehole effect equation takes into account the borehole diameter of 95 mm (Fig. 9b) and a borehole fluid, equal to 10 Ω m (field measurements). The resistivity variations are not modified after the application of the borehole correction equation.

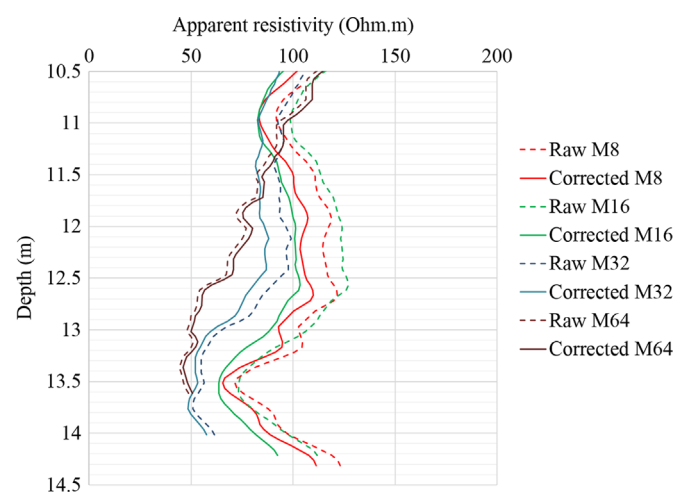

Fig. 10. Raw and corrected data of the borehole B6 for the four electrode spacing.

However, there is a general translation towards lower resistivities. This translation is minimum in the lower part of the log and then increases to around 13 m. The assumption is that the translation depends on the nature or the properties of the material. The correction M64 is insignificant due to the large spacing.

4.3. Interpretation of results

The noise calculated on the experimental site was below 1%. This value was determined by calculating a variation coefficient on the measurements made in a same borehole with the same conditions. Consequently, variations that are above the threshold are not considered as noise. They might be associated with changes in the concrete properties (natural spatial variability) or with the presence of discontinuities along the borehole.

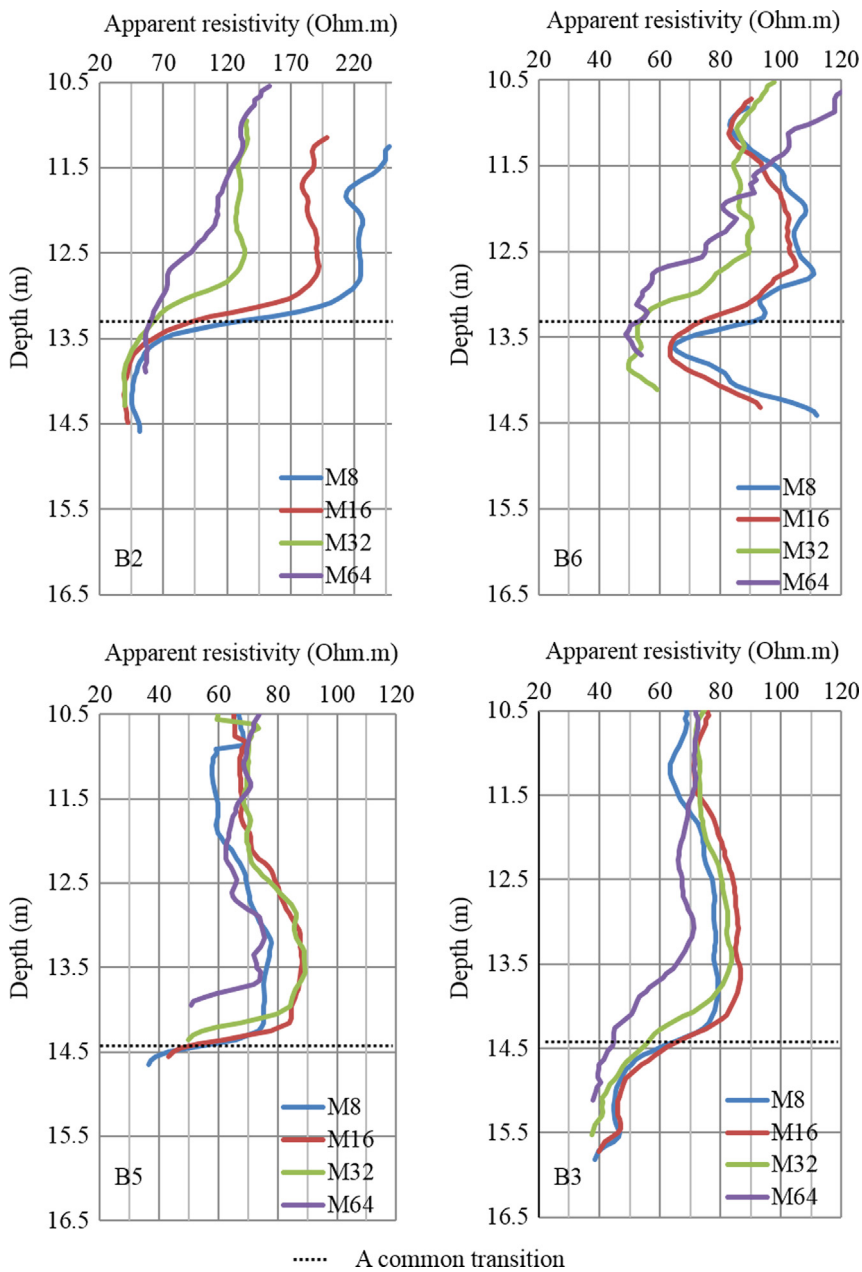

Fig. 11. Corrected results of the apparent resistivities for B2, B3, B5 and B6.

Fig. 11 shows the corrected results of the four boreholes for the four electrode spacings. The curves show similar variations on the borehole logs for the four spacings. This common transition is related either to changes in the internal properties of the material or to change in material composition. From this transition, the resistivity increases by approximately 40 to 70 Ω m (except for B2). The transition depth must be lowered by a correction equal to *AM*/2. The correct depth shows a transition around 13.4 m for B2 and B6 and around 14.5 m for B3 and B5. At 12.3 and 13.6 m, B6 shows a relative decrease of the resistivity. In modeling, this variation indicates the presence of a discontinuity. The cause of the observed changes cannot be determined without additional information.

5. Discussion

The equation of borehole effect was applied to correct the field data. A 3D representation of corrected field data after inversion data was performed (Fig. 12).

The inversion method shows two zones along the borehole. A transition at a depth of 14.5 m for B3 and B5 and at 13.4 m for B2 and B6 is observed. There is a 1-m drop between the boreholes near the embankment (B2 and B6) and the boreholes near the canal (B3 and B5). The transition is a change of resistivity between a conductive medium (Zone 1) and a less conductive medium (Zone 2).

The zones interpretation for B3 and B5 is biased because of the canal proximity. The apparent resistivities obtained by the M16, M32 and M64 spacings are biased by canal proximity, and are influenced by the resistivity of the water. Therefore, the resistivity values should not be considered as exact without further correction, but resistivity variations are still accurate. B2 and B6 are boreholes away from the canal. They present uninfluenced data by the canal water. The analysis of apparent resistivity in zone 2 (Fig. 11) shows that the measures near borehole in B2 are higher than B6. The interpretation of true resistivity values is different. However, given the lock state i.e. the saturation degree and the

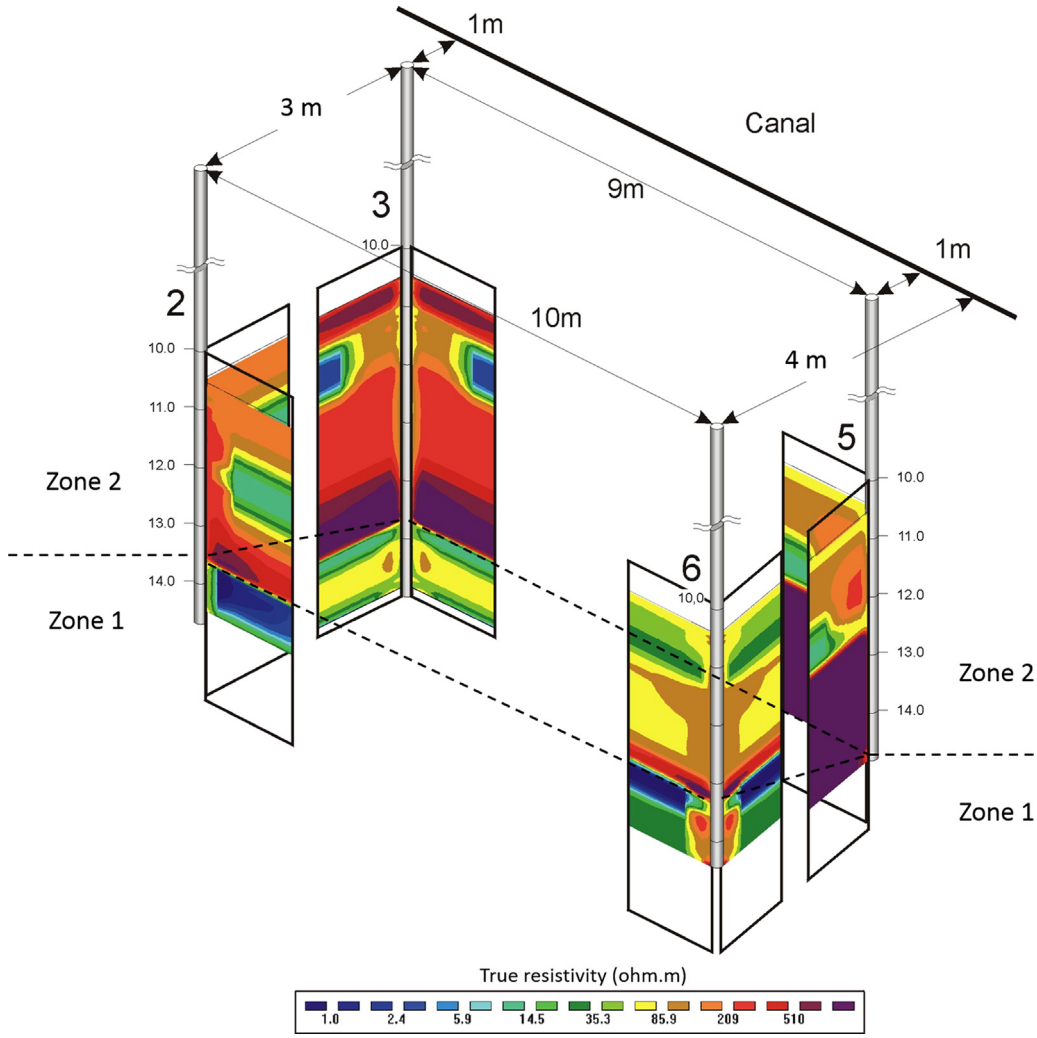

Fig. 12. 3D-inversed images on the experimental site.

age, B6 appears to have resistivity values more consistent. Therefore, more detailed interpretation will be realized about B6.

This representation allows combining the four spacings information and dividing the field into several zones. The true resistivity must be determined by an interpretation in parallel of inverted and apparent data for each spacing. The environment around boreholes should be taken into account. This method cannot be used as the only method to interpret the field investigation. In addition, the inversion has not revealed the presence of discontinuity. Therefore, a study of apparent resistivity variations is chosen to determinate the presence of discontinuities in the field.

Fig. 13 represents the corrected apparent resistivity changes with previous data obtained from the acoustic image logging (ABI-40) and optical imaging logging (OBI-40). ABI-40 acoustic Televiewer is a borehole acoustic scanner that generates an image of the borehole wall from ultrasound pulses transmitting from a rotating sensor. The tool records the amplitude and the travel time of the signals reflected at the interface between mud and formation (borehole wall). OBI-40 Optical Televiewer is a tool that generates a continuous oriented 360° image of the borehole wall using optical imaging system.

At the low part of corrected apparent resistivity log, a change is observed for the four curves. The transition depth is the inflection point depth lowered by a correction equal to $AM/2$ (Fig. 13). The transition depth is then localized at −13.4 m. Moreover, it has been mentioned that variations indicated by the four spacings show a change in the electrical properties. This transition corresponds to the transition between zone 1 and zone 2 observed on the 3D-inversed images. It has been identified with acoustic logging and imaging logging as the contact between the bedrock and the concrete structure. Therefore, zone 1 is the bedrock foundation (the highly fractured Utica shale) and zone 2 is the concrete structure.

The comparison between the apparent resistivity logs versus the acoustic and optical logs showed that the M8 spacing detects discontinuities at −13.6 and −12.3 m (Fig. 13). At −13.6 m, a resistivity decrease is identified by the four spacing. The assumption is that the probe detects a thin conductive layer. However, at this depth, the acoustic and optical measurements detect two sub-horizontal cracks and a sub-vertical crack. In reality, in the electrical logging, the thin conductive units (layers, cracks or joints) with thicknesses less than the spacing can be detected but their own characteristics are not achieved. Serra [4] defines by an equivalent layer with a thickness at least equal to the used spacing and consists of these thin conductive units. The response of the equivalent layer is the sum of contributions from each unit versus their volume percentage and their characteristic. Thus, at −13.6 m, the set of cracks is identified as an equivalent layer with a thickness equal to 0.30 m and an apparent resistivity between 50 and 70 Ω m.

At −12.3 m, the acoustic and optical logs show that the very short normal (M8) detects a concrete joint. The electrical response

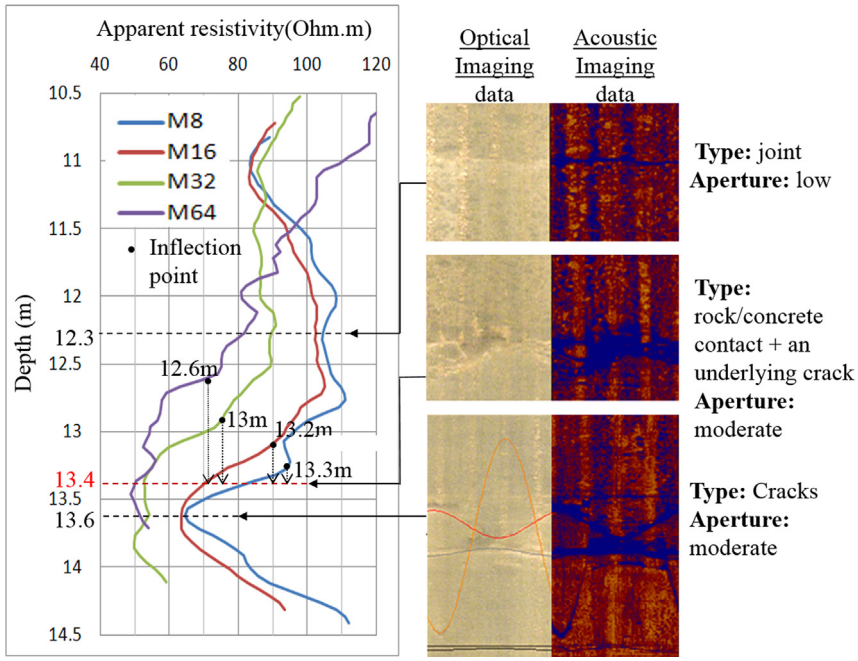

Fig. 13. Corrected apparent resistivity versus depth, imaging data and acoustic data for the borehole 6.

identifies an equivalent layer with a thickness equal to 0.20 m and an apparent resistivity equal to 103 Ω m. The configuration of this layer is a horizontal and infinite crack between two concrete layers. A preliminary quantification is performed using the modeling data and assumptions. The apparent resistivity peak is compared with the true resistivity to obtain a relative variation. At this depth and for the M8 spacing, the true resistivity of concrete is equal to about 110 Ω m. The corrected apparent resistivity observed in Fig. 13 is equal to about 103 Ω m. The relative variation is 6%. In a first approach, the crack resistivity is equal to the borehole fluid resistivity i.e. 10 Ω m. Therefore, $C_{t/c}$ is equal to about 10. Referring to modeling data that are summarized in Fig. 6, the joint aperture is estimated at 4 ± 1 mm. This result could be prudently considered as an estimation "in first approach". The hypothesis on the crack resistivity equals the fluid resistivity in the hole is arguable but represent a manner to have a minimum value for the crack aperture. Indeed, the cracks resistivity is in fact a complex contribution of all the elements constituting the crack that is to say fluids, contacts concrete–concrete, contacts concrete–fluids, all varying in thickness. As long as concrete′s resistivity is higher than the fluids resistivity one can suppose that the true resistivity of the complex system "crack" is higher than fluid′s resistivity and lower than concrete′s resistivity. Furthermore, this representation very simplistic do not consider the fact that resistivity of fluids in the crack could be different than resistivity of fluid in the hole; or else the resistivity of contact concrete–concrete in the crack could differ according the contact is done between the concrete matrix, or between aggregates. All the system is very complex to represent, and the electrical properties emerging are function of electrical resistivity of each phases, as well as geometrical parameters (apertures, roughness…). Anyway, the hypothesis done on the crack resistivity leads to an estimation of the minimum aperture. A less contrasted crack electrically, has to be more largely opened to create the same effect on the apparent resistivity recording.

The comparison between the corrected apparent resistivity versus the acoustic and optical imaging data shows that the normal electrical probe is sensitive to an isolated horizontal infinite joint, a set of cracks and interfaces. An interface is represented by a transition phase of a resistivity, characteristic of a zone, to a resistivity of another zone. A set of cracks and an isolated joint have been identified as an equivalent layer with a different intensity (resistivity). By modeling and field data, a preliminary quantification was conducted about a concrete joint.

6. Conclusion

The works show new developments to improve the characterization of massive concrete structure. The methods use the normal resistivity probe used classically in borehole logging. We focused on horizontal interfaces, as construction joint, or crack in concrete. This paper shows that the normal electrical probe detects damage zones and characterizes centimeter or millimeter cracks with infinite extension.

The modeling of a homogeneous, isotropic and infinite medium traversed by a borehole allowed developing a specific equation for the probe to correct the borehole effects on resistivity recording. The correction of this bias leads to improve the resistivity measurement reliability. The fine characterization of damage characteristics could then be studied.

In a cracked medium (horizontal interface), the modeling shows that the tool response is sensitive to the aperture and the resistivity contrast of an isolated and infinite crack. For a contrast less than 2, an aperture less than 5 mm cannot be detected. For contrast greater than 5, cracks with aperture greater than 1 mm could be detected.

The inversions of modeling and field data have shown that the method was able to identify large domains of resistivity, thin conductive layers and cracks with high contrasts. The analysis of the concrete structure cannot depend solely on the inversion method because of an imposed mesh. The apparent resistivities have shown that variations above the field noise are significant to the presence of discontinuities. The combination between the apparent resistivity and the true resistivity allows quantifying the crack aperture, assuming that the crack resistivity was equal to the borehole fluid resistivity and that the crack is infinite.

This paper emphasizes the method effectiveness to locate, detect and characterize isolated cracks. It also shows that the normal electrical probe detects a set of cracks as a thin conductive layer.

Extensive studies about the quantification of the aperture and resistivity cracks are underway. Other aspects are also taken into account i.e. the extension and the inclination of cracks.

Acknowledgements

Financial support has been provided by the Natural Sciences and Engineering Research Council of Canada (NSERC) and by the Fonds Québécois de Recherche sur la Nature et les Technologies (FQRNT)

The authors are also grateful to D. Charbonneau for his assistance regarding field work.

References

[1] Breysse D, Abraham O. Méthodologie d'évaluation non destructive des ouvrages en béton armé. Presses ENPC; 2005.
[2] Lataste JF, Sirieix C, Breysse D, Frappa M. Electrical resistivity measurement applied to cracking assessment on reinforced concrete structures in civil engineering. NDT and E Int 2003;9;36(6):383–94.
[3] Roy A, Apparao A. Depth of investigation in direct current methods. Geophysics 1971;36(5):943–59 (10/01; 2013/02).
[4] Serra O. Diagraphies différées—Bases de l'interprétation, Tome 1: Acquisition des données diagraphiques. Paris: ElfExploration; 1979.
[5] Desbrandes R. Diagraphies dans les sondages. Paris: Editions Technip; 1982.
[6] Al'Pen LM. On the solution of the fundamental problem of resistivity logging. Sci Rep, Izv Geophys Ser 1964:236–8.
[7] Tikhonov VI, Zakharov YEV. Solution of electrical prospecting for inhomogeneous media. Izv Phys Solid Earth 1977;13:833–9.
[8] Daniels J. Interpretation of buried electrode resistivity data using a layered earth model. Geophysics 1978;43(5):988–1001 (08/01; 2013/03).
[9] Gianzero S, Anderson B. An integral transform solution to the fundamental problem in resistivity logging. Geophysics 1982;47(6):946–56 (06/01; 2013/02).
[10] Zhang G, Shen L. Response of a normal resistivity tool in a borehole crossing a bed boundary. Geophysics 1984;49(2):142–9 (02/01; 2013/02).
[11] Yang F, Ward S. Inversion of borehole normal resistivity logs. Geophysics 1984;49(9):1541–8 (09/01; 2013/01).
[12] Ulugergerli EU. Two dimensional combined inversion of short- and long-normal dc resistivity well log data. J Appl Geophys 2011;2;73:130–82 2011;2;73:130–8.
[13] Guo TR, Tong LT, Chiang LW, Yang CH. A fracture study by using bipole–bipole cross-well logging. J Appl Geophys 2011 10;75(2):203–10.
[14] Whittington HW, McCarter J, Forde MC. The conduction of electricity through concrete. Mag Concr Res 1981;33(114):48–60.
[15] Archie GE. The electrical log as an aid in determining some reservoir characteristics. Dallas meeting 1942:54–62.
[16] Atkins ER, Smith GH. The significance of particle shape in formation resistivity factor–porosity relationships. J Pet Technol 1961;13(3):285–91.
[17] Snyder D, Merkel R. Analytic models for the interpretation of electrical surveys using buried current electrodes. Geophysics 1973;38(3):513–29 (06/01; 2013/03).
[18] Asch T, Morrison H. Mapping and monitoring electrical resistivity with surface and subsurface electrode arrays. Geophysics 1989;54(2):235–44 (02/01; 2013/01).
[19] Hallenburg JK. Geophysical logging for mineral and engineering applications. PennWells; 1984.
[20] Telford WS, Geldart LP, Sheriff RE. Applied geophysics. Cambridge University Press; 1990.
[21] Roy A, Dhar R. Radius of investigation in dc resistivity well logging. Geophysics 1971;36(4):754–60 (08/01; 2013/02).
[22] Mount Sopris Instrument editor. 2PEA-1000 and 2PEA-1000/F PolyElectric probes. Mount Sopris Instrument CO ed. U.S.A: Golden CO; 2002.
[23] Mount Sopris Instrument editor, MSlog v.6 for the MGX II. Mount Sopris Instrument Co., Inc.; 1998.
[24] Comsol. Comsol multiphysics user's guide—version 4.0a; 2008–2010.
[25] Bertrand Y. La prospection électrique appliquée aux problèmes des Ponts et Chaussées. Ministère de l'équipement, Laboratoire central des Ponts et Chaussées ed. Paris; 1967.
[26] Denis A, Marache A, Obellianne T, Breysse D. Electrical resistivity borehole measurements: application to an urban tunnel site. J Appl Geophys 2002;50(3):319–316 2002;50(3):319–31.
[27] Wait JR. Electromagnetic waves in stratified media. New York: Pergamon Press; 1970.
[28] Schlumberger. Abaque Gen-8 – Recueil d'abaques – Edition. 1977.
[29] Scott JH. A FORTRAN algorithm for correcting normal resistivity logs for borehole diameter and mud resistivity. Geological Survey 1978; Open-File Report 78-669.
[30] Anderson B, Minerbo G, Oristaglio M, Barber T, Freedman B, Shray F. Modeling electromagnetic tool response. Schlumberger: Oilfield Re 1992;4:22–32.
[31] Loke MH, Barker RD. Rapid least-squares inversion of apparent resistivity pseudo-sections by a quasi-Newton method. Geophys Prospect 1996;44(1):131–52.
[32] Geotomo Software. Rapid 2-D Resistivity & IP inversion using the least-squares method. 8th ed. 2013.